Dynamical and thermodynamical causes of large-scale changes in the hydrological cycle over North America in response to global warming

Richard Seager *

Lamont Doherty Earth Observatory of Columbia University, Palisades, New York

David Neelin ,

Department of Atmospheric Sciences, University of California at Los Angeles, Los Angeles, California

Isla Simpson, Haibo Liu, Naomi Henderson, Tiffany Shaw, Yochanan Kushnir, Mingfang Ting

Lamont Doherty Earth Observatory of Columbia University, Palisades, New York

Benjamin Cook

NASA Goddard Institute for Space Studies, New York, New York

* *Corresponding author address:* Richard Seager, Lamont Doherty Earth Observatory of Columbia University, 61 Route 9W., Palisades, NY 10964. Email: seager@ldeo.columbia.edu

Submitted to *Journal of Climate* February 2014. LDEO Contribution Number xxxx.

ABSTRACT

The mechanisms of model-projected atmospheric moisture budget change across North America are examined in simulations conducted with 24 models from the Coupled Model Intercomparison Project Five. Modern day model budgets are validated against the European Centre for Medium Range Weather Forecasts Interim Reanalysis. In the winter half year transient eddies converge moisture across the continent while the mean flow wets the west from central California northward and dries the southwest. In the summer half year there is widespread mean flow moisture divergence across the west and convergence over the Great Plains that is offset by transient eddy divergence. In the winter half year the models project drying for the southwest and wetting to the north. Changes in the mean flow moisture convergence are largely responsible across the west but intensified transient eddy moisture convergence wets the northeast. In the summer half year widespread declines in $P - E$ are supported by mean flow moisture divergence across the west and transient eddy divergence in the Plains. The changes in mean flow convergence are related to increases in specific humidity but also depend on changes in the mean flow including increased low level divergence in the southwest and a zonally varying wave that wets the west and east coasts in winter and dries the southwest. Increased transient eddy fluxes occur even as low level eddy activity weakens and arise from strengthened humidity gradients. Full explanation of North American hydroclimate changes will require explanation of mean and transient circulation changes and the coupling between the moisture and circulation fields.

1. Introduction

North American hydroclimate is marked by stark contrasts with semi-arid to arid regions in the southwest, wet subtropical, temperate and continental climates to the east and north and the Great Plains characterized by a remarkably strong west to east dry to wet transition. All model-based analyses of the impacts of rising greenhouse gases on North American climate project that these contrasts are to get even more marked in the coming century. This occurs as part of a general amplification of existing patterns of hydroclimate with subtropical regions, including southwest North America, getting drier and expanding poleward, and mid-latitude regions, including the northern reaches of the U.S. and Canada, getting wetter (Held and Soden 2006; Intergovernmental Panel on Climate Change 2007; Neelin et al. 2006, 2013; Seager et al. 2007; Seager and Vecchi 2010; Seager et al. 2013; Wehner et al. 2011). The simplest part of this change is the impact of the rise in specific humidity that follows the rise in saturation specific humidity driven by atmospheric warming. In regions of low level mean flow convergence this will cause an increase in precipitation minus evaporation, $P-E$, and a decrease in $P-E$ in regions of low level mean flow divergence. This process increases $P-E$ in the Intertropical Convergence Zone and in the regions of eddy-driven mean flow ascent in the mid-latitudes and decreases $P-E$ in the subtropics. It is often referred to as the "wet-get-wetter, dry-get-drier" or "rich-get-richer, poor-get-poorer" mechanism (Chou and Neelin 2004; Held and Soden 2006; Chou et al. 2009). However, changes in atmospheric circulation, in particular the poleward expansion of the Hadley Cell and poleward shift of storm tracks are also important (Previdi and Liepert 2007; Seager et al. 2010; Scheff and Frierson 2012).

The purpose of this paper is to thoroughly examine CMIP5 model-projected changes over North America and to determine the mix of dynamical and thermodynamical mechanisms that cause the spatially and seasonally varying changes. We have recently completed such an analysis for the Mediterranean region (Seager et al. (2014), hereafter S14) and this is a companion paper in the sense that the analyses are largely the same as used there (albeit on a 24 model ensemble here as opposed to the earlier 15 member ensemble). Recently Sheffield et al. (2014) and Maloney et al. (2014) have examined North America climate and climate

change in the CMIP5 multimodel ensemble. Unlike those comprehensive papers, the present paper is more focused on mean hydroclimate and extends that work by analyzing in detail the mechanism of moisture budget change within a 24 model ensemble. Further, Neelin et al. (2013) have examined the CMIP5 models' projection of increasing precipitation over California in the December through February season. This appears to differ from the projections in the earlier CMIP3 but California lies between regions of greenhouse gas-induced wetting to the north and drying to the south. These are robust projections in both model ensembles but robust predictions are in general challenging at boundaries between large-scale wetting and drying tendencies.. Neelin et al. (2013) suggest that circulation change involving an eastward extension of the strong part of the subtropical jet, and associated change in storm-track rainfall over the eastern Pacific, was responsible for the mid-winter wetting in CMIP5. The detailed moisture budget analyzed here will address this by considering mechanisms of $P - E$ change across all of North America.

Although climate models indicate human-induced hydroclimate change should already be underway across North America, it is likely currently masked by natural variability of climate. The ongoing drought in western North America, for example, is likely highly influenced by natural decadal variability, especially in the Pacific Ocean, as well as internal atmospheric variability (Hoerling et al. 2010; Seager and Vecchi 2010; Hoerling et al. 2014). Similarly a strong trend towards wetter conditions in the northeast U.S. cannot be easily attributed to human-induced climate change and instead is likely influenced by natural climate variability (Seager et al. 2012b). Despite ongoing climate variability, there is little doubt that, across North America, human-induced hydroclimate change will intensify and need to be adapted to. However, adaptation efforts will be greatly aided by narrowing of uncertainties in hydroclimate projections. Water resources in the southwest U.S. are one example. The Colorado River draws most of its flow from its northern headwaters that lie close to a nodal region between drying to the south and wetting to the north and this, and other reasons, cause considerable uncertainty in projections of future flow, though the consensus is that it will decline (Vano et al. 2014). Similarly the uncertainty about winter precipitation changes in California (Neelin et al. 2013) leads to uncertainty in changes in Sierra Nevada winter snowpack - another critical element of southwest water resources (see

MacDonald (2010) and Cayan et al. (2010) for more discussion).

Determining the uncertainty in the projections requires not just analysis of the variation among the model projections but also an assessment of why the changes occur. We then need to consider whether the physical mechanisms of model-projected hydroclimate change are properly representing processes in the real climate system or, alternatively, depend on some uncertain or poorly represented components of the model. Such information will not only be of use in determining uncertainties of projections but also can guide efforts to improve models and narrow uncertainties. The work presented here aims to move our understanding in this direction.

2. Reanalyses and CMIP5 model data

The climate models will be validated against the European Center for Medium Range Weather Forecast (ECMWF) ERA-I Reanalysis which covers 1979 to the recent (Berrisford et al. 2011b,a; Dee et al. 2011). ERA-I is the most recent of the ECMWF Reanalyses and, relative to its precursors, has an improved representation of the hydrological cycle due to assimilation of cloud and rain-affected satellite irradiances. It is based on an atmospheric model and reanalysis system with 60 levels in the vertical with a top level at 0.1mb, a T255 spherical harmonic representation and, for surface and grid point fields, a reduced Gaussian grid with about a 79km spacing (Berrisford et al. 2011b). However, the analyses performed here are with data archived by ECMWF on a regular 1.5 degrees grid with 37 model levels and at 6 hourly resolution. All calculations were performed as in Seager and Henderson (2013) (hereafter SH). SH provides a thorough analysis of errors introduced by choice of numerical methods and the temporal and spatial resolution of the reanalysis data (see also S14).

For the CMIP5 models (Taylor et al. 2012) we analyzed the historical simulations and future projections with the rcp85 emissions scenario. rcp85 is the high emissions end member of the scenarios and its' choice is justified by the current lack of international action to limit greenhouse gas emissions. We used all simulations of all models that were available at the time and with specific humidity and winds at adequate vertical resolution, with daily

resolution and for the time period of interest. This allowed 24 models whose details are provided in Table 1. Altogether 77 simulations were analyzed for the historical period and 50 for the future period. Moisture budgets were computed for each model simulation. An ensemble mean was then computed for each model followed by the multimodel ensemble. To create the multimodel ensemble, model data were regridded to a common $1^\circ \times 1^\circ$ grid. Identical methods were used for the models as for ERA-I and are detailed in SH. The only exception is that 6 hourly data were used for ERA-I and daily data for the models, a choice based on data availability

Since we are interested in the near term future of relevance to adaptation, we examine the future 2021-2040 period and compare this to the 1979-2005 period for which the ERA-I Reanalysis and the CMIP5 historical simulations overlap.

3. Moisture budget analysis methods

The analysis methods are those of SH where they are described in full detail. The description below is brief and closely follows that in S14. Since, the CMIP5 data archive most readily provides model data on pressure levels rather than the model native vertical grid, we will work in pressure coordinates for which the steady state moisture budget is:

$$P - E = -\frac{1}{g\rho_w}\nabla \cdot \int_0^{p_s} \mathbf{u} q dp, \tag{1}$$

where P is precipitation, E is evaporation or evapotranspiration, g is the acceleration due to gravity, ρ_w is the density of water, p is pressure and p_s its surface value, q is specific humidity and $\mathbf{u}$ the vector horizontal velocity. The notation follows that of SH and of Seager et al. (2012a) and S14 The vertical integral is performed as a sum over pressure levels so Eq. 1 is replaced with:

$$P - E = -\frac{1}{g\rho_w}\nabla \cdot \sum_{k=1}^{K} \mathbf{u}_k q_k dp_k, \tag{2}$$

where k refers to vertical level of which there are K total and dp_k is the pressure thickness of each level with the lowest level extending to p_s.

To determine the climatological budget we divide all quantities into monthly means, represented by overbars, departures from monthly means, represented by primes, and climatological monthly means represented by double overbars. Then Eq. 2 can be rewritten as:

$$\overline{\overline{P}} - \overline{\overline{E}} \approx -\frac{1}{g\rho_w}\nabla \cdot \sum_{k=1}^{K} \overline{\left(\overline{\mathbf{u}}_k\, \overline{q}_k + \overline{\mathbf{u}'_k q'_k}\right) \overline{dp}_k}. \tag{3}$$

Here the first and second terms on the right are the moisture convergence by the mean flow and submonthly transient eddies, respectively. The approximation is because of ignoring terms involving dp'_k which is acceptable (see SH).

The mean flow contribution can be broken down into a term related to mass divergence (and hence vertical motion) and a term related to advection across moisture gradients. To do this the divergence operator has to be taken inside the vertical summation which, in addition to the divergence and advection terms, introduces a surface term, viz.

$$\overline{\overline{P}} - \overline{\overline{E}} \approx -\frac{1}{g\rho_w}\left[\sum_{k=1}^{K} \overline{\left(\overline{\mathbf{u}}_k \cdot \nabla \overline{q}_k + \overline{q}_k \nabla \cdot \overline{\mathbf{u}}_k\right) \overline{dp}_k} + \nabla \cdot \sum_{k=1}^{K} \overline{\overline{\mathbf{u}'_k q'_k}\, \overline{dp}_k}\right] - \frac{1}{g\rho_w}\overline{\overline{q_s \mathbf{u}_s \cdot \nabla p_s}}. \tag{4}$$

To represent a difference between 21st Century (subscript '21') and 20th Century (subscript '20') quantities we introduce:

$$\Delta(\cdot) = (\cdot)_{21} - (\cdot)_{20}. \tag{5}$$

Substituting this into Eqs. 3 and 4 we get:

$$\Delta\overline{\overline{P}} - \Delta\overline{\overline{E}} \approx -\frac{1}{g\rho_w}\nabla \cdot \sum_{k=1}^{K} \Delta(\overline{\overline{\mathbf{u}}_k\, \overline{q}_k \overline{dp}_k}) - \frac{1}{g\rho_w}\nabla \cdot \sum_{k=1}^{K} \Delta(\overline{\overline{\mathbf{u}'_k q'_k}\, \overline{dp}_k}), \tag{6}$$

$$\approx -\frac{1}{g\rho_w}\sum_{k=1}^{K} \Delta(\overline{\left(\overline{\mathbf{u}}_k \cdot \nabla \overline{q}_k\right) \overline{dp}_k}) - \frac{1}{g\rho_w}\sum_{k=1}^{K} \Delta(\overline{\overline{q}_k \nabla \cdot \overline{\mathbf{u}}_k \overline{dp}_k})$$

$$-\frac{1}{g\rho_w}\nabla \cdot \sum_{k=1}^{K} \Delta(\overline{\overline{\mathbf{u}'_k q'_k}\, \overline{dp}_k}) - \frac{1}{g\rho_w}\Delta(\overline{\overline{q_s \mathbf{u}_s \cdot \nabla p_s}}). \tag{7}$$

Changes in the first and second terms of Eq. 7 can arise from either change in humidity, which is largely, but not entirely, a thermodynamical mechanism, or changes in the circulation, which is a dynamical mechanism (Seager et al. 2010). The thermodynamical and

dynamical mechanisms can be diagnostically determined by evaluating the relevant terms holding, first, the circulation and, second, the humidity fixed at their 20th Century climatological values. The terms related to the moisture advection and the mass divergent flow (the first and second terms in Eq. 7) are important and can be approximated as:

$$-\frac{1}{g\rho_w}\sum_{k=1}^{K}\Delta(\overline{(\overline{\mathbf{u}}_k\cdot\nabla\overline{q}_k)\,\overline{dp}_k}) \approx -\frac{1}{g\rho_w}\sum_{k=1}^{K}\overline{\overline{\mathbf{u}}}_{k,20}\cdot\Delta\left(\overline{\nabla\overline{q}_k\overline{dp}_k}\right) - \frac{1}{g\rho_w}\sum_{k=1}^{K}\nabla\overline{\overline{q}}_{k,20}\cdot\Delta(\overline{\overline{\mathbf{u}}_k\overline{dp}_k}), \quad (8)$$

$$-\frac{1}{g\rho_w}\sum_{k=1}^{K}\Delta(\overline{\overline{q}_k\nabla\cdot\overline{\mathbf{u}}_k\overline{dp}_k}) \approx -\frac{1}{g\rho_w}\sum_{k=1}^{K}\Delta(\overline{\overline{q}_k\overline{dp}_k})\nabla\cdot\overline{\overline{\mathbf{u}}}_{k,20} \;-\; \frac{1}{g\rho_w}\sum_{k=1}^{K}\overline{\overline{q}}_{k,20}\Delta(\overline{\nabla\cdot\overline{\mathbf{u}}_k\overline{dp}_k}). \quad (9)$$

Further approximation comes from ignoring terms quadratic in Δ, covariances of anomalous monthly means and from using the 20th Century values for dp_k. In Eqs. 8 and 9 the first terms on the right (the 'thermodynamic terms') involve the changes in humidity while the circulation is fixed and the second terms (the 'mean circulation dynamics' terms) involve the changes in the circulation while the humidity is fixed.

The monthly mean data were available on 17 levels and the daily data on 8 levels so the mean flow moisture convergence was evaluated on 17 levels and the transient eddy moisture convergence on just 8 levels. This does introduce some error as described in SH and S14. The main source of error is the underestimation of transient eddy moisture fluxes by use of daily, as opposed to higher time resolution, data. This error is consistent across time periods so that the difference in the moisture budget and its constituent terms can still be diagnosed in a useful way.

4. The climatological North American moisture budget in the ERA-I Reanalysis

a. The winter half year

Figure 1 shows the various terms in the North American sector climatological moisture budget according to ERA-I for the winter half year (November through April). In this half year there are P maxima along the west coast of North America and stretching across the

east from the Gulf coast to Newfoundland. $P - E$ is positive across the continent outside of the North American Monsoon region with maxima along the West Coast and the east as well. The mean flow moisture convergence (Figure 1d) is partly responsible for the West Coast maximum. In contrast transient eddy moisture flux convergence (Figure 1h) sustains the $P - E$ maximum in the east and occurs as one part of a dipole with transient eddy moisture flux divergence over the subtropical North Atlantic Ocean and south of the Gulf Stream/North Atlantic Drift. That is, during winter, storm systems pick up moisture from the ocean and converge it into the eastern part of North America (see also Shaw and Pauluis. (2012)). Transient eddies actually converge moisture across all of North America, except for eastern Mexico, with the secondary maximum along the West Coast. The negative $P - E$ over Mexico is sustained by strong mean flow moisture divergence. The part of the mean flow moisture divergence due to mass divergence (Figure 1e) is, over the Pacific and Atlantic Oceans, a fairly clear north south pattern with moisture divergence in the subtropics and convergence in the mid-latitudes, consistent with Hadley Cell descent and eddy-driven mid-latitude ascent. This simple pattern is not so clear over land where it is likely that vertical motion induced by topography interrupts this pattern.

In the winter half year, P is clearly related to the storm tracks, both directly via transient eddy moisture flux convergence and indirectly via mean flows (with mid-latitude low level convergence and subtropical low level divergence) induced by eddy momentum transports. The wettest regions are therefore the Pacific Northwest at the tail end of the Pacific storm track and the eastern parts of North America impacted by the Atlantic storm track. With storm tracks much weaker over land, the interior parts of North America are drier as well as the more southern latitudes equatorward of the storm track. The near all-continent transient eddy convergence of moisture can be understood, in part, as a consequence of cold temperatures and very low humidities over the continent which allows eddies to essentially diffuse moisture in from the warmer and moister atmosphere over adjacent oceans. It is notable that, in the mean, it is only the eddies that allow for positive $P - E$ in southwest North America where the mean flow diverges moisture. It is worth noting for later reference that in the Eastern Pacific, and along the North American West Coast from Oregon poleward, there is a substantial role for mean flow moisture convergence in maintaining the climatological

precipitation associated with the storm track region. This breakdown between transient and mean flow terms in cooperatively maintaining a continuous precipitation feature may be likewise noted in earlier budgets of National Center for Environmental Prediction (NCEP) and NCEP2 reanalysis (Newman et al. 2012). Advection and convergence by the zonal component of the mean flow converges moisture that had been transported poleward by transient terms further west in the storm track.

b. The summer half year

In the summer half year (Figure 2) the pattern of P across North America has a general wet east-dry west pattern in contrast to the more wet north-dry south pattern of the winter half year. This reflects the weakening and poleward shift of the storm tracks and the development of subtropical anticyclones. The wet regions are now far western Canada and the eastern regions from the Gulf of Mexico and northwards east of the Appalachians. Much of this P is compensated for by E such that, in fact, $P - E$ is negative - that is, there is atmospheric moisture divergence - across most of North America except for southern Mexico, the Pacific Northwest, northeastern Canada and the southeast U.S. Moisture export is therefore still occurring in regions where the summer is the wetter of the two half years. This is possible since a portion of the evaporated water fell as precipitation in the preceding winter half year when E was very low.

In contrast to the all-wetting pattern of the winter half year, transient eddies in the summer converge moisture all along the west coast from Baja California north and over northeast North America, but diverge moisture from most of Mexico, the Great Plains and the southeast U.S (Figure 2h, see also Shaw and Pauluis. (2012)). This is likely related to eddies acting diffusively on the strong meridional moisture gradients that develop in summer (see below). The summer half year mean flow moisture convergence dries the west coast south of Seattle and moistens it north of there and also provides a notable wetting tendency for the central Plains. Advection of the moisture field (Figure 2f) is an important part of the mean flow moisture convergence and also adopts the east-west wetting-drying contrast. This is related to moistening in the central U.S. by southerly flow within the

western flank of the Atlantic subtropical high, particularly concentrated within the Great Plains Low Level Jet (see also Shaw and Pauluis. (2012)), and drying by northerly flow across western North America on the eastern flank of the North Pacific subtropical high. The aridity of southwestern North America is therefore seen to originate from being south of the Pacific storm track in winter and on the eastern, descending northerly flow, side of a subtropical high in summer. In contrast the humid conditions across eastern North America arise from being influenced by the Atlantic storm track in winter and being on the western, ascending southerly flow, side of a subtropical high in summer.

5. Climatological North American moisture budget in the CMIP5 models

Figures 3 and 4 show the CMIP5 multimodel mean climatological moisture budget terms.

Looking at the winter half year first (Figure 3), to first order, the models do a highly creditable job reproducing the ERA-I budget as seen in Figure 1. Locations of P and $P-E$ maxima are quite well modeled. The models have positive $P-E$ across the entire continent, in agreement with observations except over most of Mexico. The multimodel mean, however, has P too great over the southwest (including southern California) which also translates into excess E. The models sustain positive $P-E$ across the continent due in large part to transient eddy moisture convergence (Figure 3h) although this appears weaker than in observations (because of the use of daily, as opposed to higher time resolution, data, see SH and S14). The models also agree with observations that the mean flow diverges moisture across most of the continent but converges it over the Pacific Northwest. Contributions of the advective and mass divergent components to this are also in good agreement with the ERA-I patterns.

In the summer half year (Figure 4) the models do a credible job of reproducing the ERA-I P pattern albeit with too little P over the southern Plains and U.S. Southeast and too small of a dry region in the southwest U.S. The models agree with ERA-I that there is moisture export (though it is underestimated) from the continent (negative $P-E$) except for the far

northwest and northeast and southern Mexico. The models also agree with ERA-I that the export is sustained by mean flow moisture divergence across the west and transient eddy moisture divergence in the southern and central Plains (Figures 4d and h) with the mean flow converging moisture into the latter region due to moisture advection (from the south, Figure 4f).

These comparisons of modeled to ERA-I moisture budgets suggest that the models, with some exceptions, are successfully simulating key processes of importance to North American hydroclimate, both qualitatively and quantitatively. Perfect agreement should not be expected for a few reasons. First, diagnostic computation of budgets from model data archives introduces error. Principal amongst these is an underestimation of the transient eddy moisture fluxes and convergence due to use of daily (as here) data as opposed to higher resolution or, ideally, time step data (see SH for more on this). That underestimation is clear in these comparisons here. Further, ERA-I covers a particular period that, due to decadal variability, may not be representative of the long term climatology. Also the models do not have the spatial resolution to fully capture the influences of the complex topography of North America on hydroclimate.

6. Projected near-term future changes in North American hydroclimate

a. Projected hydroclimate changes in the winter half year

Figures 5 shows the change for 2021-2040 relative to 1979-2005 in the winter half year of the CMIP5 multimodel mean moisture budget. In the winter the change in P is largely north-south with wetting to the north and drying to the south over Mexico and the interior southwestern U.S. E, following warming, increases everywhere except for Mexico such that the change in $P-E$, while also largely zonal, has a border between wetting and drying that is further north than that of P alone. However, there are some interesting zonal asymmetries with, particularly, the west coast of the U.S. down to central California experiencing a wetting change (Neelin et al. 2013) and a tongue of drying change extending northward

in the interior southwest U.S. The regions of notable wetting under climate change are the Pacific northwest and the northeast U.S. and eastern Canada.

Causes of the $P-E$ change arise from changes in both the mean flow and transient eddy moisture convergence. The change in transient eddy moisture flux convergence (Figure 5h) is concentrated over central and eastern North America where it represents a strengthening of the northward transport with increased divergence (drying) to the south, primarily over the Atlantic Ocean, and convergence (wetting) to the north over the north central and eastern U.S. and central to eastern Canada. The change in transient eddy moisture convergence also represents a northward shift of the 20th Century pattern. In contrast, across western North America the wetting-drying, north-south, pattern is sustained by a north-south pattern of mean flow moisture convergence-divergence (Figure 5d). A predominantly zonally-symmetric component of this is associated with the mean mass divergence term (Figure 5e) while the component related to advection of humidity (Figure 5f) introduces zonal asymmetries with wetting at the coast of southwest North America, drying in the interior southwest, and wetting again at the east coast of the U.S. The changes in $P-E$ are governed by the same processes as the climatological $P-E$ with transients governing over eastern North America and the mean flow over western North America. The drying tendency over the Caribbean has contributions from both the mean and transients, each reasonably continuous with features affecting North America.

b. Projected hydroclimate changes in the summer half year

In the summer half year (Figure 6) P is projected to decrease across most of Mexico and across the U.S. from the Pacific coast to the Appalachians and increase over Canada and the eastern U.S. (Figure 6a). General increases in E, except across the year-round drying areas in the south of North America, causes, in combination with the changes in P, net summer drying (negative $P-E$ change) across almost the entire continent except for the core of the northern reach of the North American Monsoon region, Alaska and the far northwestern and northeastern parts of Canada. This is, like the winter half year, a roughly north-south wetting-drying pattern.

Unlike for the winter, in the summer half year the change in transient eddy moisture flux convergence (Figure 6h) plays an important role, drying to the south and wetting to the north. The transient drying is particularly strong in the central and northern Plains and midwest. The dominant role of the change in mean flow moisture convergence (Figure 6d) is to dry the western third of the U.S. and southwestern Canada as well as provide a strong drying in the Caribbean region. The change in mean flow moisture convergence also moistens the North American Monsoon region which is offset partially by increased transient eddy moisture divergence. Both the components associated with mass divergence (Figure 6e) and moisture advection (Figure 6f) contribute to the change in mean flow moisture convergence across western North America and Mexico. When this breakdown is performed, this drying is offset by the surface term (Figure 6g) which includes orographic precipitation from flow up topography.

c. Robustness of projected changes in P and $P - E$

The moisture budget calculations performed here were for the 24 models that made all the needed data available. However, the multimodel mean patterns of $P - E$ and its change are very similar to those in a larger 35 model ensemble ashown here (see `http://kage.ldeo.columbia.edu:81/SOURCES/.LDEO/.ClimateGroup/.PROJECTS/.IPCC/.CMIP5/.MultiModelStatistics/`). To further check the robustness of the model-projected changes, in Figure 7 we show the number of the 24 models that agree on the sign of the change and have the same sign change as the multimodel mean. Values are only plotted where more than three quarters of the models agree in this way. For winter half year P, there is substantial model agreement on increased P across the northern U.S. and Canada from coast to coast and decreased P in Mexico, the Caribbean and the far interior southwest U.S. For winter half year $P-E$ the model agreement on the southwest drying region extends further into the U.S. than the agreement on P alone. Model agreement on an increase in $P - E$ in northern regions of the U.S. and Canada is less than for P alone, presumably because E increases and offsets the increase in P. In the summer half year there is widespread model agreement on an increase of P across Canada and a decrease of $P - E$ across the

central to northern U.S. and southern Canada.

d. Contribution of humidity change and mean circulation change to the changes in mean flow moisture convergence

So far we have shown that the changes in North American hydroclimate under global warming involve changes in both the mean flow and transient eddy moisture convergence. However the changes associated with the mean flow could arise from either changes in specific humidity even in the absence of a change in mean flow (the so-called 'thermodynamic' component) and, or, changes in mean flow even in the absence of a change in the specific humidity (the so-called 'mean circulation dynamics' component), as well as a nonlinear term involving changes in both mean flow and humidity which is found to be small. Therefore we break down the changes in mean flow moisture convergence as in Eqs. 7 and 8 and show the results in Figures 8 and 9 for the winter and summer half years, respectively.

Perhaps the simplest component is that due to the change in specific humidity combining with the unchanged mass divergent flow and this is shown in the top right of Figure 8 for the winter half year. This is the term invoked by Chou and Neelin (2004), Held and Soden (2006) and Chou et al. (2009) to explain an in-place intensification of spatial patterns of $P - E$, the so-called "rich-get-richer, poor-get-poorer", or "wet-get-wetter, dry-get-drier" mechanism. Although changes in circulation can influence humidity change (see below), at its simplest, this term arises from a general increase in specific humidity as the atmosphere warms. This allows for an increase in mean flow moisture convergence (divergence) where the low level mean flow is convergent (divergent). This term causes a tendency to increased $P - E$ in the tropics and high latitudes (where the mean low level flow is convergent) and a decrease in the subtropics (where the low level mean flow is divergent). Over the continent the rise in specific humidity causes drying over parts of interior southwest North America and wetting over the west coast from central California north in the winter season (Fig. 8b). This "rich-get-richer" term is the leading drying effect in the Caribbean, partially offset by other terms.

Despite the popularity of the "rich-get-richer" mechanism for explaining hydroclimate

change, the winter drying tendency in parts of southwest North America occurs due to the change in the mass divergent flow (Figure, upper left). This term does not have the simple zonal symmetry and north-south contrast of the part of the thermodynamic term associated with mass convergence and, instead, must reflect some more complex adjustment of the mean flow field. The unchanged mean flow advecting the change in specific humidity (Figure 8, bottom left) provides a quite complex and fine scale $P - E$ tendency over the east Pacific and North America which reflects to a large extent the complexity of the spatial pattern of low level humidity change (see below). The change in moisture advection due to the change in advecting flow (Figure 8, bottom right) creates a zonally-varying wave like pattern with negative $P - E$ tendency in the central Pacific, Mexico, the interior southwest U.S. and the central Atlantic, and a positive $P - E$ tendency over the east Pacific and west and east coasts of the U.S. The causes of this wave pattern in $P - E$ tendency will be examined below.

In the summer half year the increase in specific humidity combining with the unchanged mean flow (Figure 9, top right) causes widespread drying across the far west of North America where the low level mean flow is divergent within the subsiding branch of the North Pacific subtropical high. The component due to the change in the mass divergent mean flow (Figure 9, top left) causes a strong drying tendency over Mexico and the southern to central Plains and also over the Pacific northwest and northeast Pacific but with a wetting tendency over the subtropical North Pacific. Both these terms (Figure 9 top) contribute to the drying over the Caribbean. Advection of the change in specific humidity (Figure 9, bottom left) causes a drying tendency over almost all of western North America but a wetting tendency over the North Pacific and the southern Plains. In the summer half year advection of the unchanged humidity field (Figure 9, bottom right) by the changed mean flow provides a wetting tendency over the interior southwest and central North America.

7. Relating the projected changes in North American hydroclimate to changes in circulation and specific humidity

From the previous analysis it is clear that changes in the mean flow are important to explaining changes in North American hydroclimate. It also appears that changes in the spatial patterns of the specific humidity field may be important. We will examine each in turn.

a. Changes in the sub-monthly transient eddy field

Figure 10 shows the climatology and change in the upper and lower tropospheric, sub-monthly, meridional velocity variance, $\overline{v'^2}$, a measure of storm track activity for the winter and summer half years. At upper levels during the winter half year the change is primarily a poleward shift of the eddy activity. There is a decrease (order 5%) in $\overline{v'^2}$ over southwest North America and a weaker increase over more northerly areas of North America. The northward shift of the Atlantic eddy activity is also clear. In contrast to the upper level poleward shift, the lower level eddy activity decreases everywhere across North America and the surrounding oceans (in agreement with Chang et al. (2012)). The poleward shift of upper level eddy activity is also clear across the Pacific, North America and the Atlantic in the summer half year. In this season eddy activity decreases across the entire U.S., Mexico and southern Canada. This decrease is also apparent at lower levels, again consistent with Chang et al. (2012). The changes in upper troposphere eddy activity are also broadly consistent with the changes in high-pass filtered 250mb height variance shown by Lau and Ploshay (2013) for a simulation with a high resolution Geophysical Fluid Dynamics Laboratory model, with the exception that that model did not have a decrease over southwest North America in the DJF season analyzed.

It is notable that the upper level transient eddy activity shifts poleward at all longitudes and year-round despite the changes in zonal winds (i.e. the jet stream) being more longitudinally varying, implying the lack of a one-to-one coupling between these. This is consistent

with an analysis of changes in the tropospheric zonal momentum budget by Simpson et al. (2014). They show that, while the changes in zonal winds induced by a rise in greenhouse gases are quite variable in space, the driving by the high-pass filtered transient eddy activity is more zonally symmetric and would, in general, act to shift the jets poleward. That this does not occur at all longitudes and seasons is because of important momentum fluxes by the stationary components of the flow.

The main feature of change in winter half year transient eddy moisture convergence - the wetting over northeastern North America and drying over the subtropical Atlantic Ocean - although appearing as an amplification of the pre-existing pattern, is not a result of a stronger storm track. Instead it probably arises because the mean moisture gradient within which the eddies operate is stronger (see below). On the other hand the northward shift of the transient eddy convergence-divergence couplet over the western Atlantic-eastern North America may be explainable in terms of the northward shift of the upper level storm activity. In the summer half year the main feature is the increased transient eddy moisture divergence from the central Plains. This also occurs within an environment in which the low level eddy activity has weakened and, therefore, must also be a response to the change in the mean humidity field.

b. Changes in the mean flow field

Turning to the changes related to the mean flow, to analyze the change in advection, in Figure 10 we also show the change in 850mb geopotential height from which the change in low level flow can be inferred assuming geostrophy. The 20th century climatological heights are also shown. For the winter half year the 850mb height change shows a relative low centered over the Aleutian Islands in the North Pacific and a relative high over the central mid-latitude North Atlantic. Noting that heights increase everywhere due to atmospheric warming, the change over the Atlantic might easily be interpreted as a northward extension of subtropical high pressure but, over the Pacific, the change appears as deeper low pressure on the eastern flank of, and to the south of, the Aleutian Low. Southerly flow on the eastern flank of the strengthened Aleutian Low correlates well in space with a wetting tendency by

the anomalous flow advecting the unchanged humidity field (Figure 8). Also, anomalous southeasterly flow around the anomalous central North Atlantic high correlates well in space with the wetting tendency over eastern North America due to changes in mean flow advecting the unchanged humidity field (Figure 8). In between these coastal features, advective drying by a changed circulation is associated with northerly flow to the west of a Caribbean low. It is notable how far these height changes deviate from a simple zonal mean change.

The changes in heights and circulation in the summer half year are more simple and characterized by a northward expansion of the North Pacific and Atlantic subtropical highs. $P-E$ tendencies over the oceans due to changes in moisture advection induced by the mean flow changes (e.g. drying over the northeast Pacific) can be explained in terms of these changes in heights but, as noted earlier, in the summer half year the associated changes over land are small.

c. Changes in the mean specific humidity field

To complete the description of hydroclimate change over North America, Figure 11 shows both the climatology and the change in the vertically integrated specific humidity field for the summer and winter half years. In the winter half year the change is to a large extent an amplification of the existing pattern. This follows from an assumption of approximately fixed relative humidity which, together with the nonlinear dependence of saturation humidity on temperature, implies, for a uniform temperature change, a larger increase of humidity in warmer and moister regions than in cooler and drier regions. However, the pattern of humidity change deviates from this simple relation in that there is a striking maximum extending from the Caribbean northeastward over the subtropical to mid-latitude western Atlantic Ocean and another weaker tongue extending northward from the subtropical Pacific Ocean to western North America. These maxima in humidity increase are separated by a tongue of minimum increase over western North America. The winter season maxima and minima in the specific humidity increase can be explained in terms of the change in meridional winds and inferred from Figure 10. However, to make this even clearer, in Figure 12 we show the winter half year change in low level (850mb) and upper level (250mb) meridional velocity.

The southerly flow change at the coasts are seen with northerly flow change in-between over southwest North America. Further, it is seen that this change in the mean flow is contained within a cross-northern hemisphere wave train that appears to originate from the subtropical northwest Pacific. The origins of this approximately barotropic wave train, which is quite robust across the models (as shown by the stippling in Figure 12; also the robustness and amplitude of this wave amplifies as the century progresses (not shown)), are not clear but its importance to North American hydroclimate change is obvious.

8. Conclusions and discussion

a. Conclusions

We have conducted a comparison of the atmospheric moisture budget over North America and surrounding ocean areas between a CMIP5 multimodel ensemble and the ERA-I Reanalysis and then examined how this changes in the models between the last several decades and the period of 2021-2040. The purpose is to understand the physical mechanisms that cause well known model projected changes in $P - E$, especially the drying of southwest North America, the wetting of northern regions and the summer half year continent-wide seasonal drying. The conclusions are as follows:

- According to ERA-I, the winter half year is the moisture supply season for most of North America with positive $P - E$ everywhere except Mexico. The transient eddies dominate the atmospheric supply of moisture to the continent. The mean flow provides further moisture supply to the Pacific Northwest and diverges moisture from southwest North America. In the summer half year most of the continent except for far northern and southern regions, loses moisture to the atmosphere. This is despite many parts of North America having summer precipitation maxima (which must be allowed for by the greater summer evapotranspiration). The summer half year atmospheric moisture divergence is accomplished by the mean flow across the western U.S. and by transient eddies in the central U.S. which offset a mean flow wetting tendency. Transient eddies in the summer continue to provide a wetting tendency to the west coast of the U.S.

and Canada and New England and eastern Canada. These essential features of North American hydroclimate are captured by the multimodel mean of 24 CMIP5 models. Transient eddy moisture convergence in the models as estimated here is lower than in ERA-I, almost certainly due to the use of daily as opposed to higher time resolution data (see Seager and Henderson (2013)).

- In the winter half year the models project that Mexico, the interior southwestern, and southern U.S. will experience drying as measured by a decrease in $P - E$ that comes from a drop in P and, in the more northerly reaches of drying, an increase in E. The models project $P - E$ to increase over the more northern portion of North America (roughly north of $35 - 40°N$). The southwestern and southern winter season drying is balanced by an increase in the mean flow moisture divergence. The wetting in northeastern North America is driven by an intensification of transient eddy moisture flux convergence in the region accompanied by intensified divergence over the subtropical North Atlantic Ocean.

- The models project summer drying and atmospheric moisture export to intensify across almost the entire continent associated with increased mean flow moisture divergence across western North America and increased transient eddy moisture divergence in the central U.S.

- In the winter half year, the rise in humidity combining with the unchanged divergent flow tends to intensify $P - E$ patterns with the primary effect over the continent of generating a wetting tendency over the west coast of North America from central California northward.

- In the summer half year this term causes a widespread drying tendency over the west coast of North America and parts of Mexico and the Caribbean where the low level mean flow is divergent. Year round increased low level mass divergence causes a drying tendency across Mexico, the southwest U.S. and the Caribbean. The change in mean flow also causes, in the winter half year, advective wetting tendencies at the west and east coasts of North America with drying over southwest North America. This zonally-

varying pattern of advective drying and wetting tendencies is contained within a wave that appears to propagate east from the subtropical northwest Pacific Ocean region.

- The changes in transient eddy moisture fluxes are in many regions an intensification of the existing patterns that result from increasing gradients of specific humidity while the strength of eddies in the lower troposphere, as measured by sub-monthly $\overline{v'^2}$, actually weaken across much of North America. At the west coast of North America, there is a poleward shift of the winter half year storm track but changes in the mean flow contributions to $P - E$ are needed to explain the $P - E$ changes.

b. Discussion

The analysis presented here, despite the quantitative methodology, is largely descriptive of changes in model-projected North American hydroclimate change. For North America, a full explanation of hydroclimate change must account for 1) the rise in specific humidity, 2) spatial variations in the rise, 3) the changes in the divergent and non-divergent components of the mean flow and how they influence moisture divergence and advection and 4) changes in transient eddy strength, location and associated moisture convergence. In this regard a few key problems remain to be solved:

i. Why do the mid-latitude storm tracks shift poleward in the future and, at lower levels, weaken? The shift has received much attention. A review of explanations, and a new one in terms of the tropospheric response to stratospheric changes, is offered by Wu et al. (2012, 2013). However, the matter is not solved, and Simpson et al. (2014) argue that changes in stationary waves are needed to explain all the zonal and seasonal variations of the mean circulation. In the same spirit, Lau and Ploshay (2013) have attributed some of the summer season zonal variations in their single model study to stationary waves forced by increasing precipitation over the eastern tropical Pacific Ocean. Chang et al. (2012) suggest that the weakening of eddy activity at low levels originates in a reduction of low level baroclinicity but this needs to be demonstrated.

ii. Drying by increased mean flow moisture divergence, even in the absence of changes

in humidity, is important for drying of southwest North America and implies a low level mass divergence change in the region. The dynamics of this e.g. whether this is a local expression of a poleward expanded Hadley Cell (as is clearly seen over the Atlantic Ocean to the east (Seager et al. 2014)), or a more local feature, need to be determined.

iii. The causes of the relatively high zonal wavenumber wave that stretches across the Pacific-North-America-Atlantic sector, wetting the west and east coasts of North America, and drying the southwest interior, needs to be determined. This appears to originate in the subtropical northwest Pacific but changes in diabatic heating, the mean flow that determines the orographic forcing, the Rossby wave source associated with heating, or the medium through which forced waves propagate, could all be, wholly or in part, responsible. Given the importance, e.g. for California, of the hydroclimate impacts of this wave this must be a priority.

iv. The decomposition provided here, though illuminating, is not definitive. For one thing the timescale separation between monthly and sub-monthly scales is quite arbitrary. Further, the separation into thermodynamic and dynamic components does not account for the coupling between the various components of the moisture budget. For example, at the west coast of North America a southerly advection change tends to increase moisture in a region where storm systems and mean flow convergence can convert it into positive $P - E$. Hence the humidity changes are, in part, induced by dynamic changes. Further, changes in the transient eddies can drive mean flow changes and associated moisture budget changes. Only a much more theoretically-informed analysis, which would push understanding of extratropical circulations to more fully account for coupling between moist processes and circulation, can provide deeper insight.

Despite these suggestions for future research the current work, based on the latest model simulations, identifies more clearly how the atmospheric branch of the hydrological cycle over North America responds to greenhouse warming. The surety of rising atmospheric humidity in a warming atmosphere results in a tendency to drying in southwest North America and wetting further north. However, it must be acknowledged that equally important model-

projected hydroclimate tendencies arise from mean and transient circulation changes that are yet to be physically explained. Understanding why these occur in models, and assessing whether, given model limitations and biases, these results are trustworthy, is key to narrowing uncertainties in projections of future hydroclimate across North America.

Acknowledgments.

This work was supported by NOAA award NA10OAR4310137 (Global Decadal Hydroclimate Variability and Change), DOE award DE-SC0005107 and NSF awards AGS-1243204 and AGS-1102838 (JDN). We would like to thank Dong Eun Lee for downloading the ERA-Interim data and ECMWF for making the reanalysis data available. We acknowledge the World Climate Research Programme's Working Group on Coupled Modelling, which is responsible for CMIP, and we thank the climate modeling groups (listed in Table 1 of this paper) for producing and making available their model output. For CMIP the U.S. Department of Energy's Program for Climate Model Diagnosis and Intercomparison provides coordinating support and led development of software infrastructure in partnership with the Global Organization for Earth System Science Portals.

REFERENCES

Berrisford, P., P. Kallberg, S. Kobayashi, D. Dee, S. Uppala, A. J. Simmons, P. Poli, and H. Sato, 2011a: Atmospheric conservation properties in ERA-Interim. *Quart. J. Royal Meteor. Soc.*, **137**, 1381–1399.

Berrisford, P., et al., 2011b: The ERA-Interim archive version 2.0. Tech. rep., European Centre for Medium Range Weather Forecasts, ERA report series No. 1, 23 pp.

Cayan, D., T. Das, D. Pierce, T. Barnett, M. Tyree, and A. Gershunova, 2010: Future dryness in the southwest United States and the hydrology of the early 21st Century drought. *Proc. Nat. Acad. Sci.*, **107**, 21 271–21 276.

Chang, E. K. M., Y. Guo, and X. Xia, 2012: CMIP5 multimodel ensemble projection of storm track change under global warming. *J. Geophys. Res.*, **117**, D23 118, doi:10.1029/2012JD018 578.

Chou, C. and J. D. Neelin, 2004: Mechanisms of global warming impacts on regional tropical precipitation. *J. Climate*, **17**, 2688–2701.

Chou, C., J. D. Neelin, C. Chen, and J. Tu, 2009: Evaluating the 'rich-get-richer' mechanism in tropical precipitation change under global warming. *J. Climate*, **22**, 1982–2005.

Dee, D., et al., 2011: The ERA-Interim Reanalysis; Configuration and performance of the data assimilation system. *Quart. J. Roy. Meteor. Soc.*, **137**, 553–597.

Held, I. M. and B. J. Soden, 2006: Robust responses of the hydrological cycle to global warming. *J. Climate*, **19**, 5686–5699.

Hoerling, M. P., J. Eischeid, A. Kumar, R. Leung, A. Mariotti, K. Mo, S. Schubert, and R. Seager, 2014: Causes and predictability of the 2012 Great Plains drought. *Bull. Amer. Meteor. Soc.*, in press.

638 Hoerling, M. P., J. Eischeid, and J. Perlwitz, 2010: Regional precipitation trends: Distin-
639 guishing natural variability from anthropogenic forcing. *J. Climate.*, **23**, 2131–2145.

640 Intergovernmental Panel on Climate Change, 2007: *Climate Change: The Physical Science*
641 *Basis*. Cambridge University Press, Cambridge, England, 365 pp.

642 Lau, N.-C. and J. J. Ploshay, 2013: Model projections of the changes in atmospheric cir-
643 culation and surface climate over North America, the North Atlantic, and Europe in the
644 Twenty-First Century. *J. Climate*, **26**, 9603–9620.

645 MacDonald, G. M., 2010: Water, climate change, and sustainability in the southwest. *Proc.*
646 *Nat. Acad. Sci.*, **107**, 21 256–21 262.

647 Maloney, E. D., et al., 2014: North American climate in CMIP5 experiments: Part III:
648 Assessment of 21st century projections. *J. Climate*, in press.

649 Neelin, J. D., B. Langenbrunner, J. E. Meyerson, A. Hall, and N. Berg, 2013: California
650 winter precipitation change under global warming in the Coupled Model Intercomparison
651 Project Phase 5 ensemble. *J. Climate*, **26**, 6238–6256.

652 Neelin, J. D., M. Munnich, H. Su, J. E. Meyerson, and C. E. Holloway, 2006: Tropical drying
653 trends in global warming models and observations. *Proc. Nat. Acad. Sci.*, **103**, 6110–6115.

654 Newman, M., G. N. Kiladis, K. M. Weickman, F. M. Ralph, and P. D. Sardeshmukh, 2012:
655 Relative contribution of synoptic and low-frequency eddies to time-mean atmospheric
656 moisture transport, including the role of atmospheric rivers. *J. Climate*, **25**, 7341–7361.

657 Previdi, M. and B. Liepert, 2007: Annular modes and Hadley Cell expansion under global
658 warming. *Geophys. Res. Lett.*, **34**, doi:10.1029/2007GL031 243.

659 Scheff, J. and D. M. W. Frierson, 2012: Robust future precipitation declines in CMIP5
660 largely reflect the poleward expansion of model subtropical dry zones. *Geophys. res. Lett.*,
661 **39**, doi:10.1029/2012GL052 910.

662 Seager, R. and N. Henderson, 2013: Diagnostic computation of moisture budgets in the
663 ERA-Interim Reanalysis with reference to analysis of CMIP-archived atmospheric model
664 data. *J. Climate*, **26**, 7876–7901.

665 Seager, R., H. Liu, N. Henderson, I. Simpson, C. Kelley, T. Shaw, Y. Kushnir, and M. Ting,
666 2014: Causes of increasing aridification of the Mediterranean region in response to rising
667 greenhouse gases. *J. Climate*, submitted (revised December 2013).

668 Seager, R., N. Naik, and G. A. Vecchi, 2010: Thermodynamic and dynamic mechanisms for
669 large-scale changes in the hydrological cycle in response to global warming. *J. Climate*,
670 **23**, 4651–4668.

671 Seager, R., N. Naik, and L. Vogel, 2012a: Does global warming cause intensified interannual
672 hydroclimate variability? *J. Climate*, **25**, 3355–3372.

673 Seager, R., N. Pederson, Y. Kushnir, J. Nakamura, and S. Jurburg, 2012b: The 1960s
674 drought and subsequent shift to a wetter climate in the Catskill Mountains region of the
675 New York City watershed. *J. Climate*, **25**, 6721–6742.

676 Seager, R., M. Ting, C. Li, N. Naik, B. Cook, J. Nakamura, and H. Liu, 2013: Projections
677 of declining surface water availability for the southwestern U.S. *Nature Climate Change*,
678 **3**, 482-486.

679 Seager, R. and G. A. Vecchi, 2010: Greenhouse warming and the 21st Century hydroclimate
680 of southwestern North America. *Proc. Nat. Acad. Sci.*, **107**, 21 277–21 282.

681 Seager, R., et al., 2007: Model projections of an imminent transition to a more arid climate
682 in southwestern North America. *Science*, **316**, 1181–1184.

683 Shaw, T. A. and O. Pauluis., 2012: Tropical and subtropical meridional latent heat trans-
684 ports by disturbances to the zonal mean and their role in the general circulation. *J. Atmos.*
685 *Sci.*, **69**, 1872–1889.

686 Sheffield, J., et al., 2014: North American climate in CMIP5 experiments. Part I: Evaluation
687 of 20th century continental and regional climatology. *J. Climate*, in press.

688 Simpson, I., T. Shaw, and R. Seager, 2014: A diagnosis of the seasonally and longitudinally
689 varying mid-latitude circulation response to global warming. *J. Atmos. Sci.*, submitted
690 (revised February 2014).

691 Taylor, K. E., R. J. Stouffer, and G. A. Meehl, 2012: An overview of CMIP5 and the
692 experiment design. *Bulletin of the American Meteorological Society*, **93**, 485–498.

693 Vano, J. A., et al., 2014: Understanding uncertainties in future Colorado River streamflow.
694 *Bull. Amer. Meteor. Soc.*, in press.

695 Wehner, M., D. R. Easterling, J. H. Lawrimore, R. R. Heim, R. S. Vose, and B. D. San-
696 ter, 2011: Projections of future drought in the continental United States and Mexico. *J.*
697 *Hydrometeor.*, **12**, 1359–1377.

698 Wu, Y., R. Seager, M. Ting, N. Naik, and T. Shaw, 2012: Atmospheric circulation response
699 to an instantaneous doubling of carbon dioxide. Part I: Model experiments and transient
700 thermal response in the troposphere. *J. Climate*, **25**, 2862–2879.

701 Wu, Y., R. Seager, M. Ting, N. Naik, and T. Shaw, 2013: Atmospheric circulation response
702 to an instantaneous doubling of carbon dioxide. Part II: Atmospheric transient adjustment
703 and its dynamics. *J. Climate*, **26**, 918–935.

List of Tables

Institute	Model	Resolution (lon x lat), level	Ensemble size	
			20thC	rcp85
Beijing Climate Center (BCC)	1. bcc-csm1-1	T42, L26	1	1
	2. bcc-csm1-1-m	T106, L26	1	1
College of Global Change and Earth System Science, Beijing Normal University (BNU)	3. BNU-ESM	T42, L26	1	1
Canadian Centre for Climate Modeling and Analysis (CCCma)	4. CanESM2	T63 (1.875°x1.875°), L35	5	5
National Center for Atmospheric Research (NCAR)	5. CCSM4	288x200 (1.25°x0.9°), L26	1	1
Centre National de Recherches Meteorologiques / Centre Europeen de Recherche et Formation Avancees en Calcul Scientifique (CNRM-CERFACS)	6. CNRM-CM5	T127(1.4°x1.4°), L31	1	1
Centro Euro-Mediterraneo per I Cambiamenti Climatici (CMCC)	7. CMCC-CM	T159, L31	1	1
Commonwealth Scientific and Industrial Research Organisation in collaboration with the Queensland Climate Change Centre of Excellence (CSIRO-QCCCE)	8. CSIRO-Mk3-6-0	T63(1.875°x1.875°), L18	1	1
Institute of Atmospheric Physics, Chinese Academy of Sciences and Tsinghua University (LASG-CESS)	9. FGOALS-g2	128x60, L26	2	1
Geophysical Fluid Dynamics Laboratory (NOAA GFDL)	10. GFDL-CM3	C48 (2.5°x2.0°), L48	2	1
	11. GFDL-ESM2G	144x90 (2.5°x2.0°), L24	1	1
	12. GFDL-ESM2M	144x90 (2.5°x2.0°), L24	1	1
Met Office Hadley Centre (Hadley Center)	13. HadGEM2-CC	192x144(1.25°x1.875°),L60	1	1
Institute for Numerical Mathematics (INM)	14. inmcm4	2.0°x1.5°, L21	1	1
Institut Pierre-Simon Laplace (IPSL)	15. IPSL-CM5A-LR	3.75°x1.875°, L39	6	3
	16. IPSL-CM5A-MR	2.5°x1.25°, L39	2	1
	17. IPSL-CM5B-LR	96x96 (3.75°x1.875°) , L39	1	1
Atmosphere and Ocean Research Institute (The University of Tokyo), National Institute for Environmental Studies, and Japan Agency for Marine-Earth Science and Technology (AORI/NIES/JAMSTEC)	18. MIROC5	T85, L40	5	3
	19. MIROC-ESM	T42, L80	3	1
	20. MIROC-ESM-CHEM	T42, L80	1	1
Max Planck Institute for Meteorology (MPI-M)	21. MPI-ESM-LR	T63, L47	3	3
	22. MPI-ESM-MR	T63, L47	3	1
Meteorological Research Institute (MRI)	23. MRI-CGCM3	TL159 (1.125°x1.125°), L48	1	1
Norwegian Climate Centre (NCC)	24. NorESM1-M	144x96 (2.5°x1.875°), L26	3	1

TABLE 1. CMIP5 models used in this study with information on host institute, resolutions (L refers to number of vertical levels, T to triangular truncation and C to cubed sphere) and ensemble sizes.

List of Figures

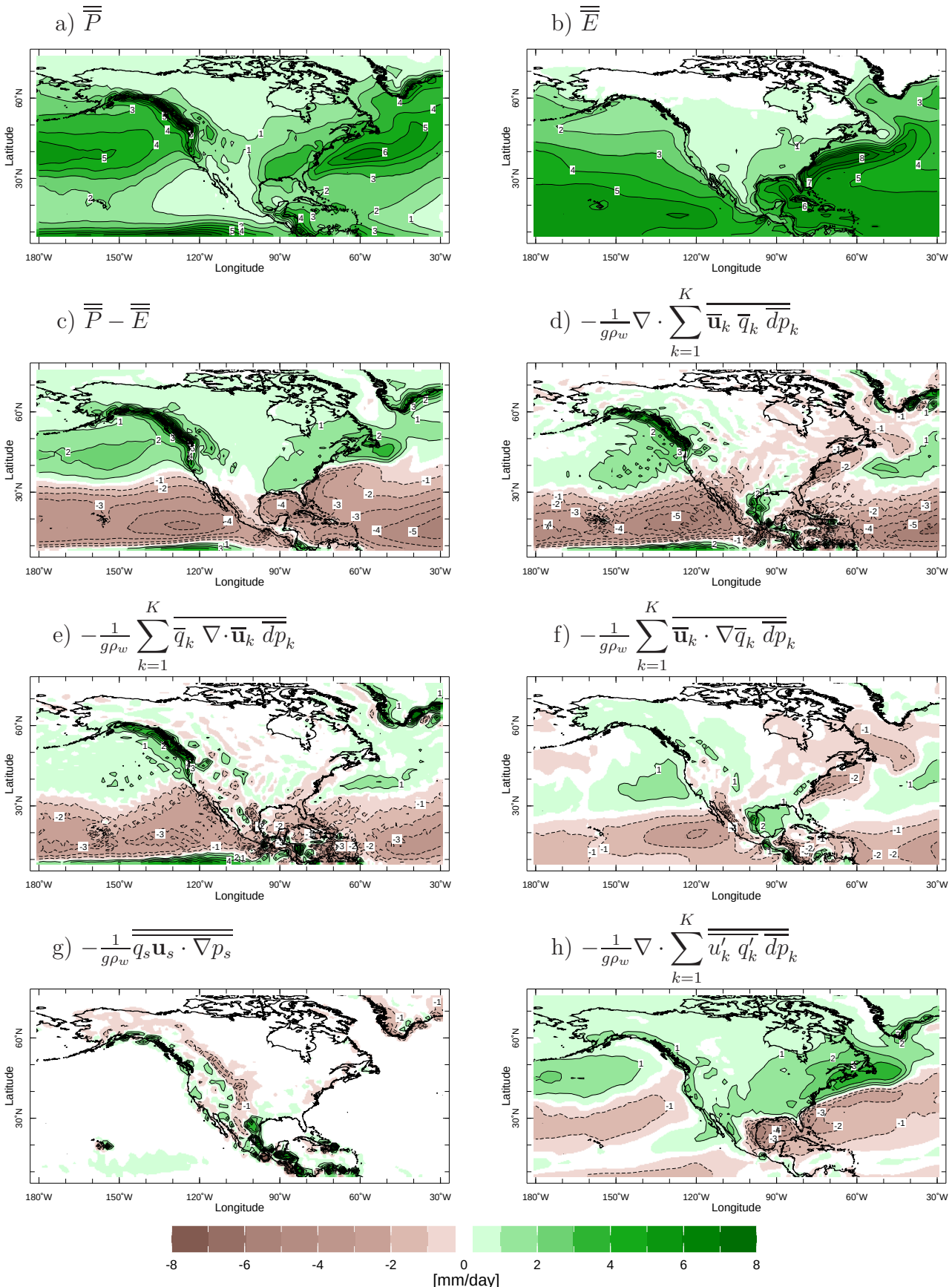

FIG. 1. The November through April half year climatological moisture budget for the North American sector from the ERA-I Reanalysis. The various panels are a) P, b) E, c) $P-E$, d) the moisture convergence by the mean flow with its components due to, e), mass divergence and, f), advection, g) the surface term and h) the transient eddy moisture convergence.

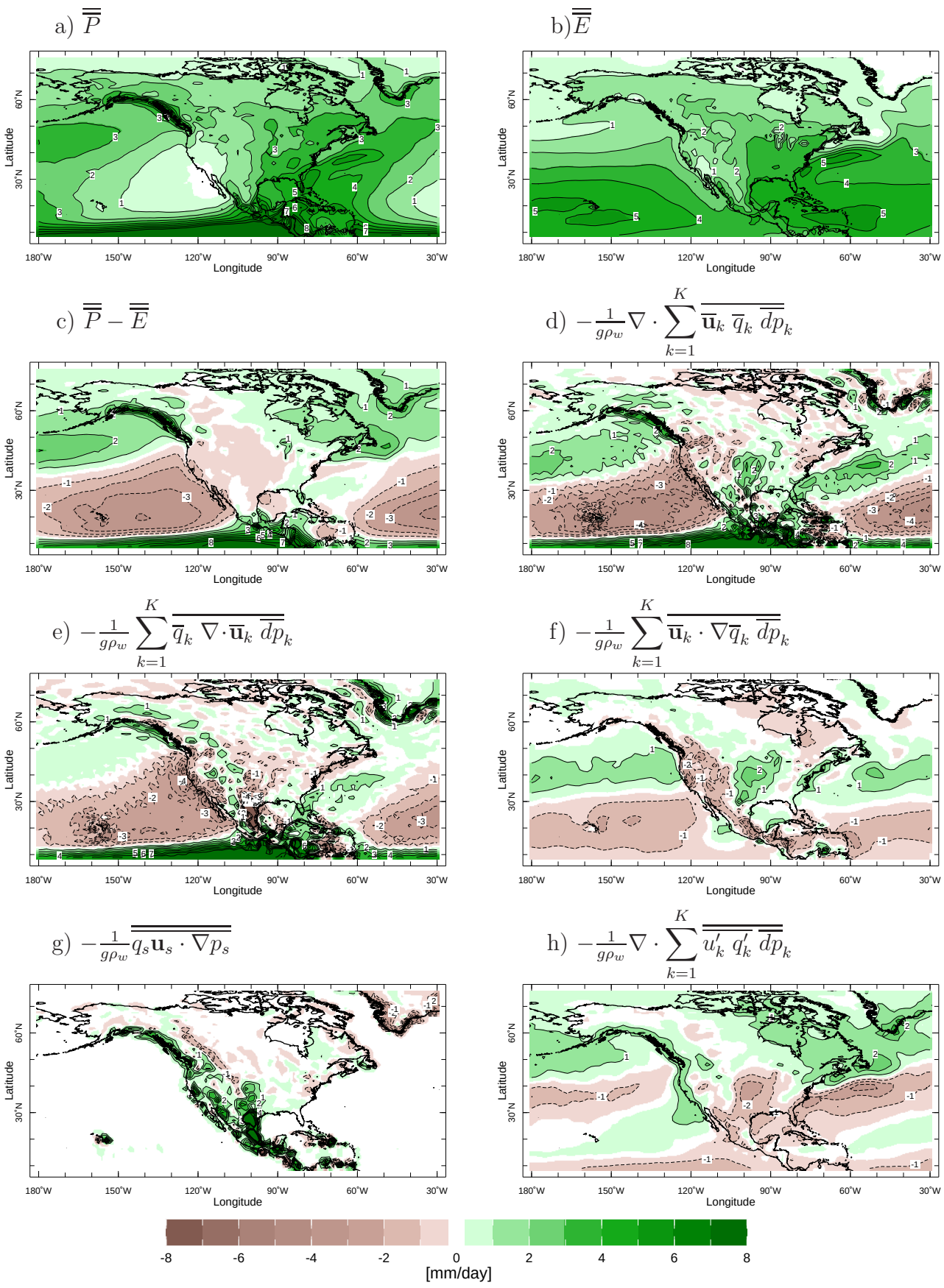

FIG. 2. Same as Figure 1 but for the May through October half year.

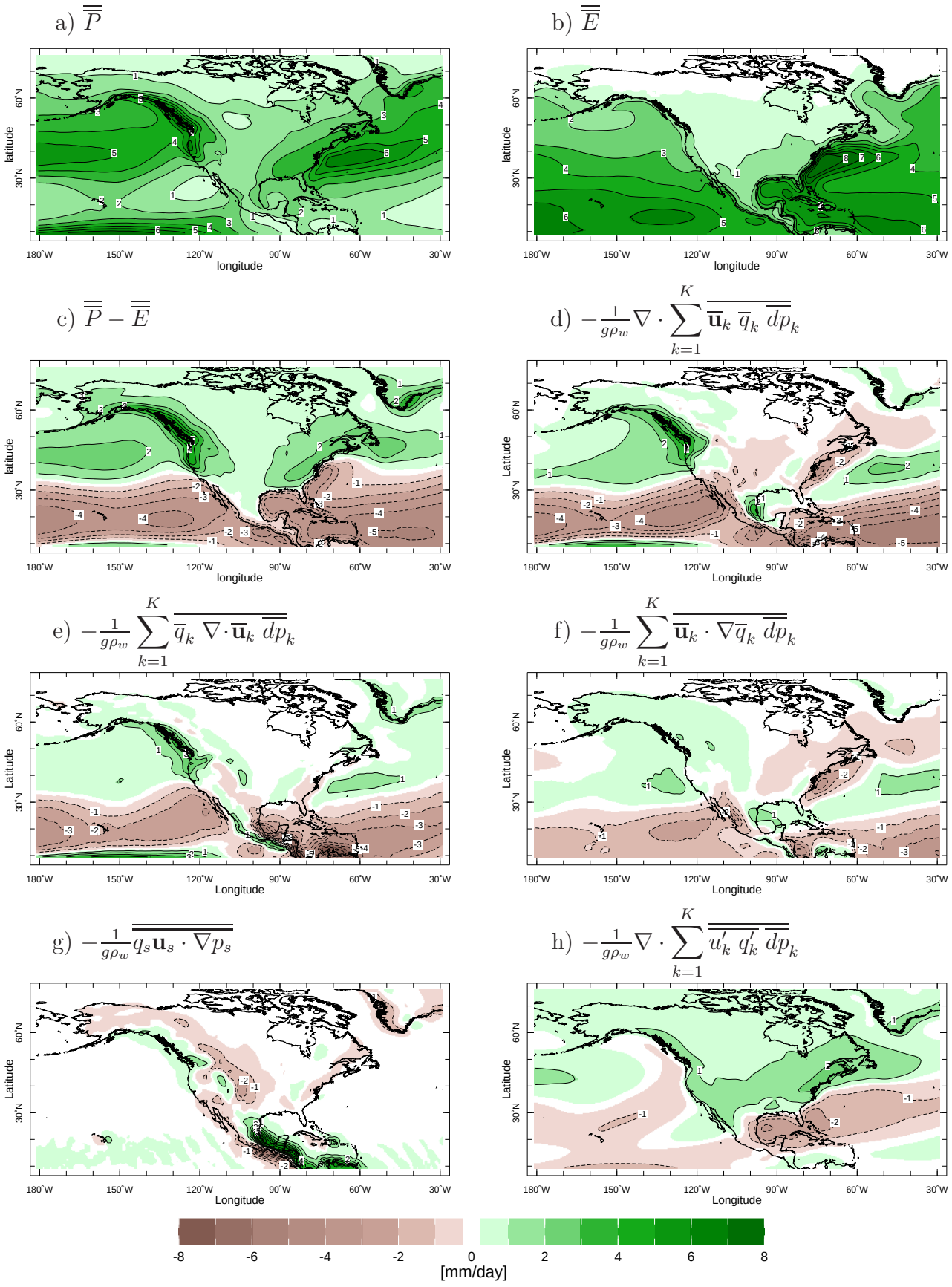

FIG. 3. Same as Figure 1 but showing the moisture budget terms for the multimodel mean of the CMIP5 models for the winter half year.

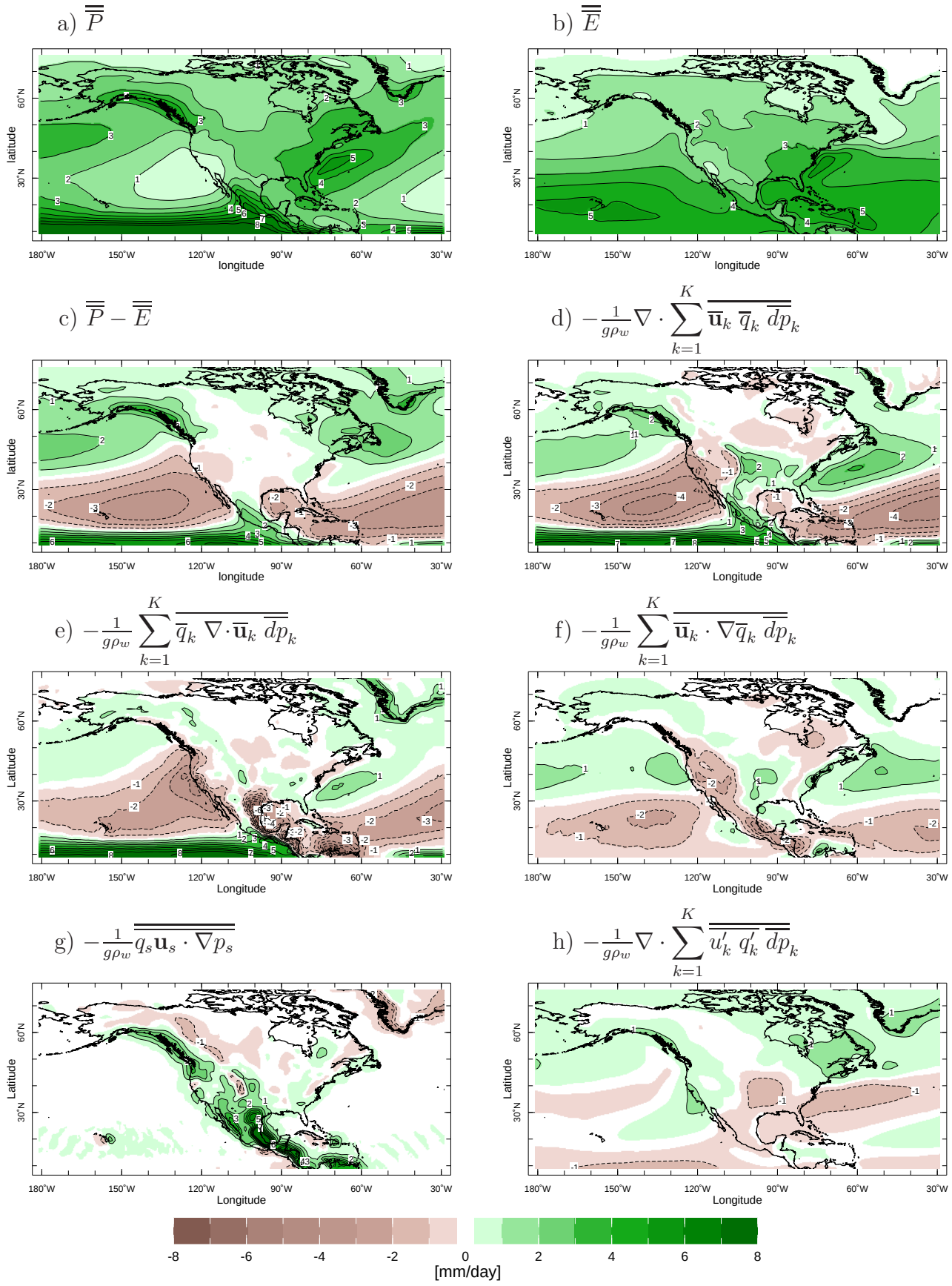

FIG. 4. Same as Figure 2 but showing the moisture budget terms for the multimodel mean of the CMIP5 models for the summer half year.

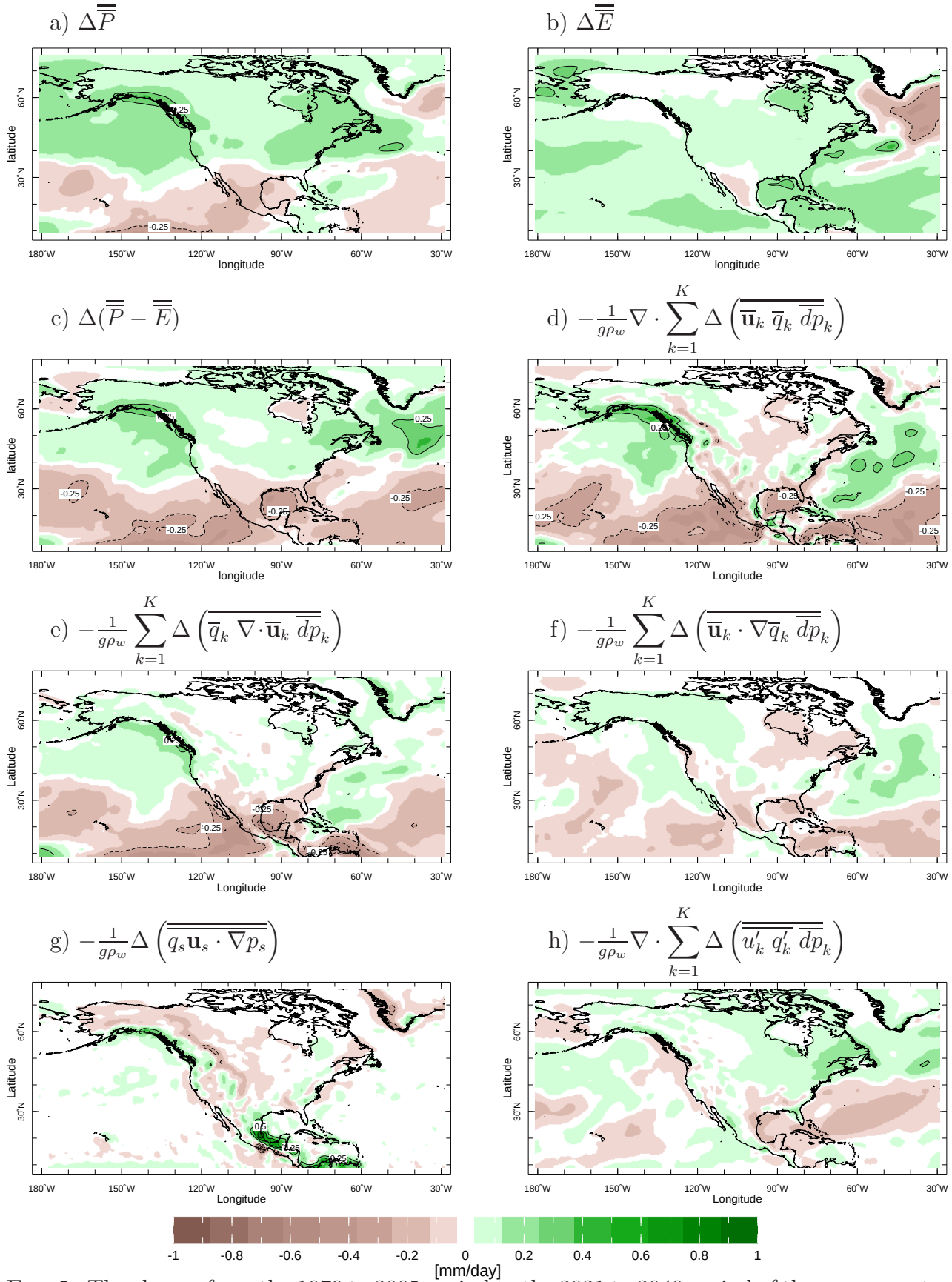

FIG. 5. The change from the 1979 to 2005 period to the 2021 to 2040 period of the component of the moisture budget for the CMIP5 multi-model mean and for the winter half year. The various panels show the change in a) P, b) E, c) $P - E$, d) moisture convergence by the mean flow with its components changes due to e) mass divergence (lower middle left) and f) advection (lower middle right), g) the surface term and h) transient eddy moisture convergence. Units are mm/day.

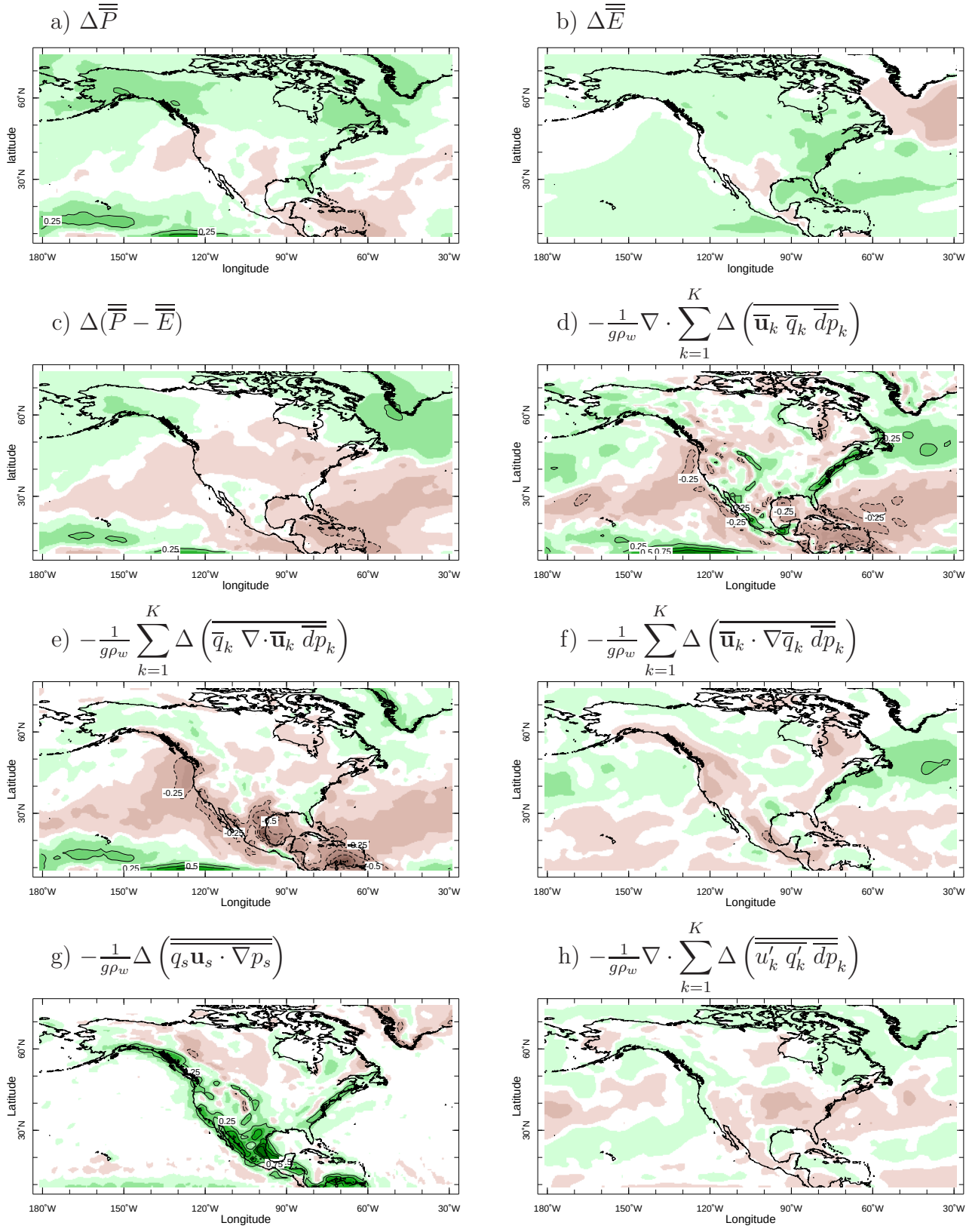

FIG. 6. As in Figure 5 but for the summer half year. Units are mm/day.

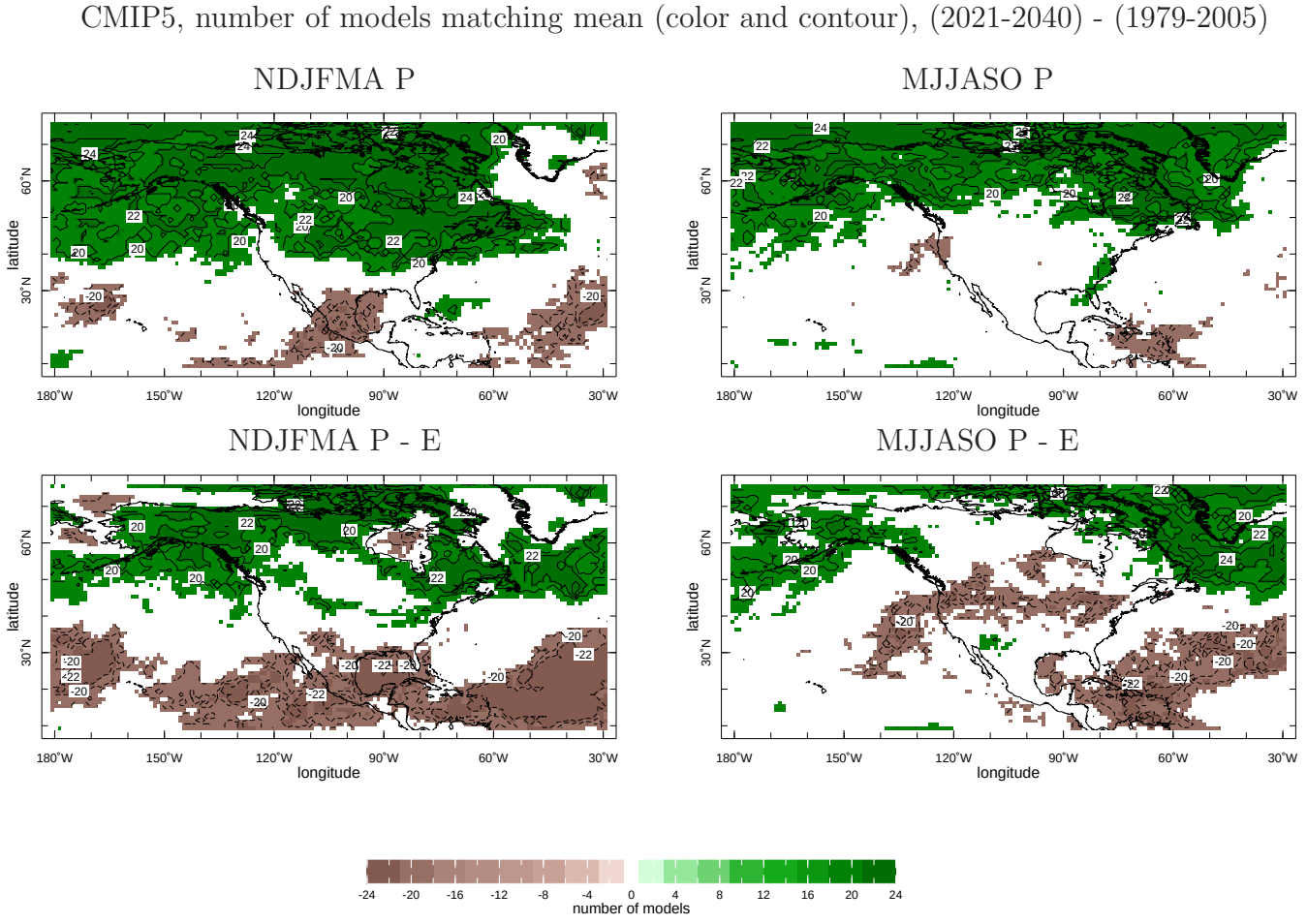

FIG. 7. The number of models that agree with the multimodel mean change in precipitation (top) and precipitation minus evaporation (below) for winter (left) and summer (right) half years. 24 models were used and values are only plotted when 18 or more (roughly three quarters) of the models agree on the sign of the change.

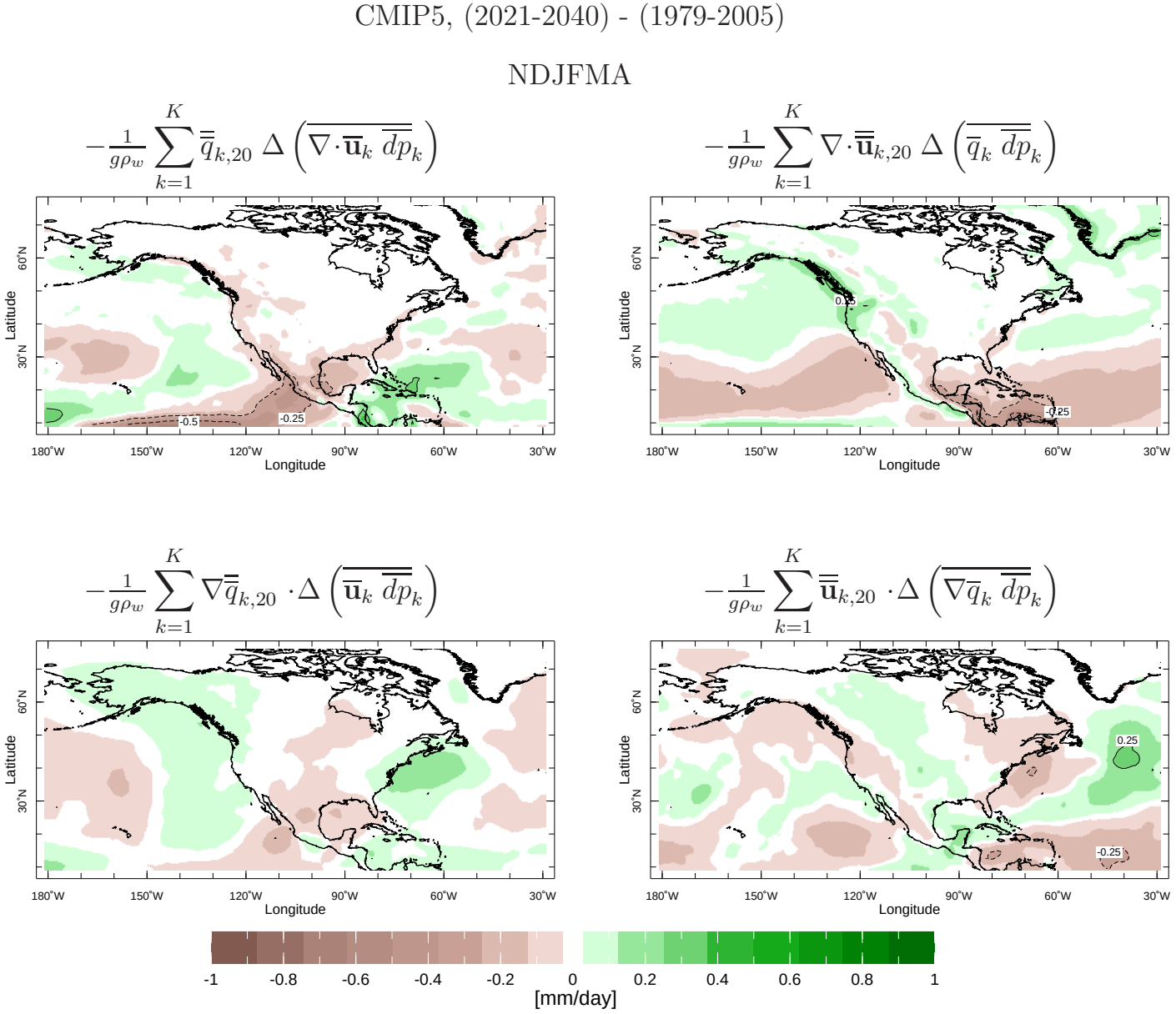

FIG. 8. The contributions to the change in the mean flow moisture convergence during the winter half year for the CMIP5 multimodel mean. The top row shows the dynamic (left) and thermodynamic (right) contributions to the component related to divergent mean flow. The lower row shows the dynamic (left) and thermodynamic (right) contributions to the component related to change in moisture advection. Units are mm/day.

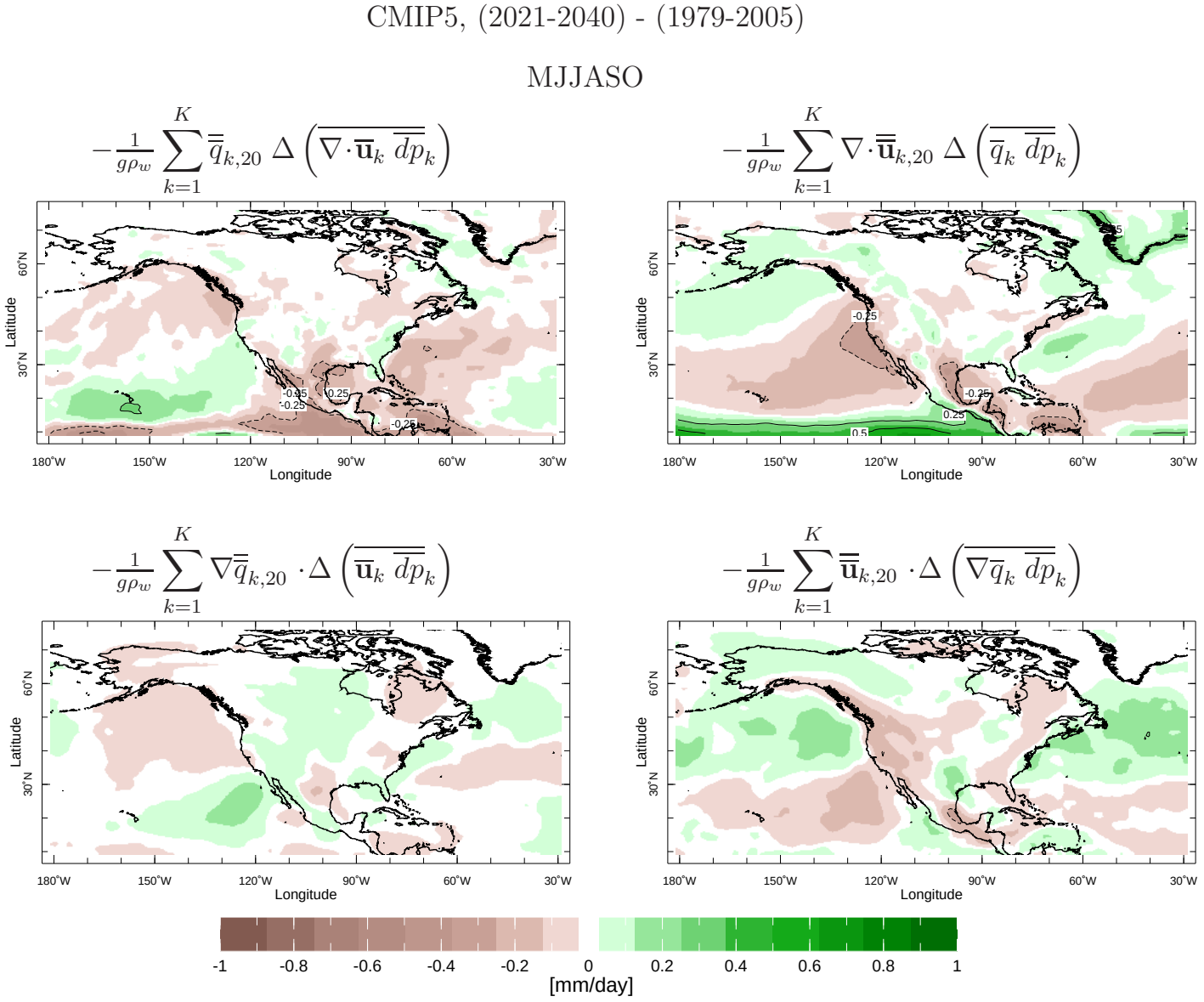

FIG. 9. Same as Figure 8 but for the summer half year.

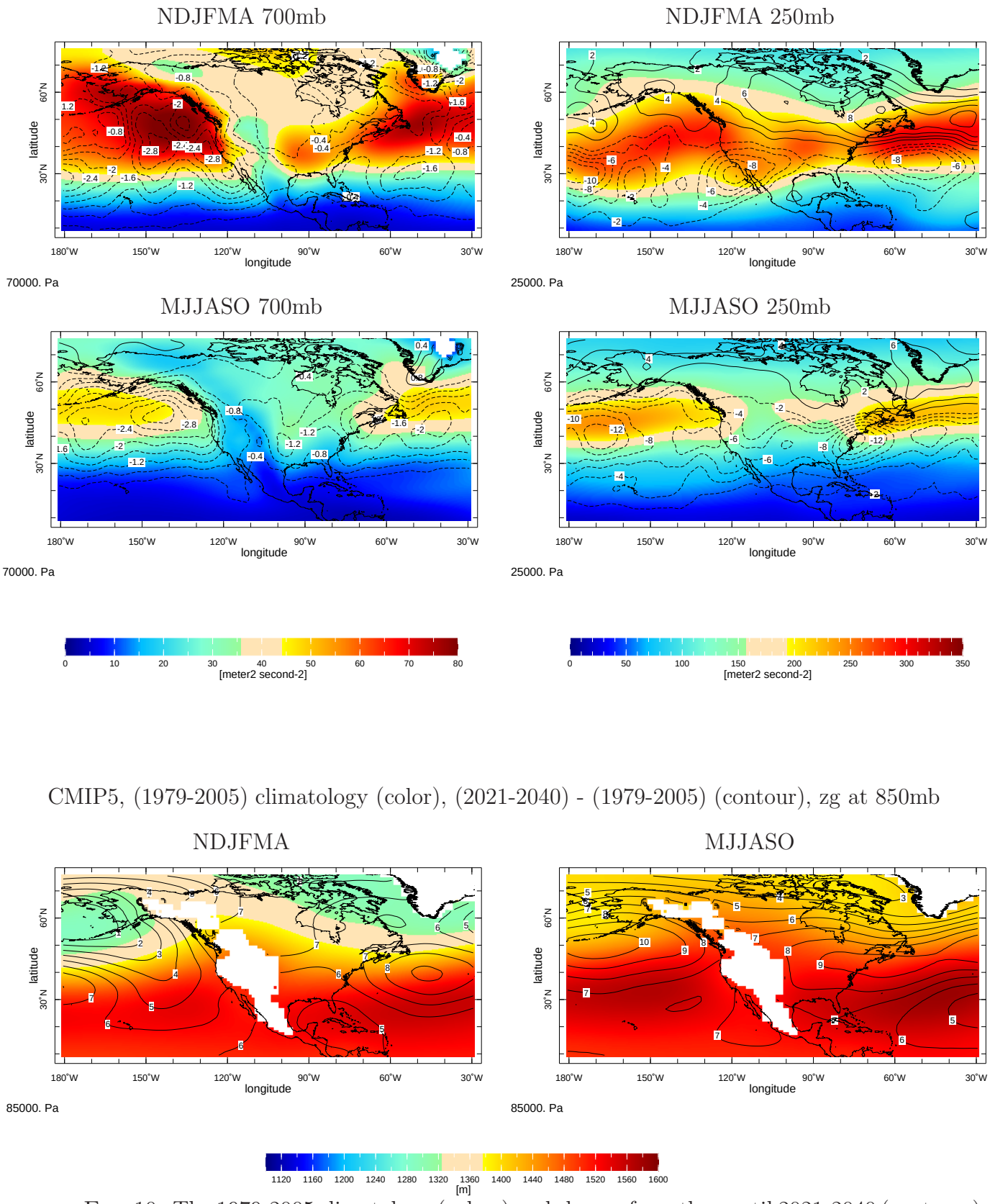

FIG. 10. The 1979-2005 climatology (colors) and change from then until 2021-2040 (contours) of the multimodel mean sub monthly meridional velocity variance at 700mb (left) and 250mb (right) for the winter (top) and summer (middle) half years and the 850mb geopotential height for the winter (bottom left) and summer (bottom right) half years. Units are $m^2 s^{-2}$ for velocity variance and m for heights.

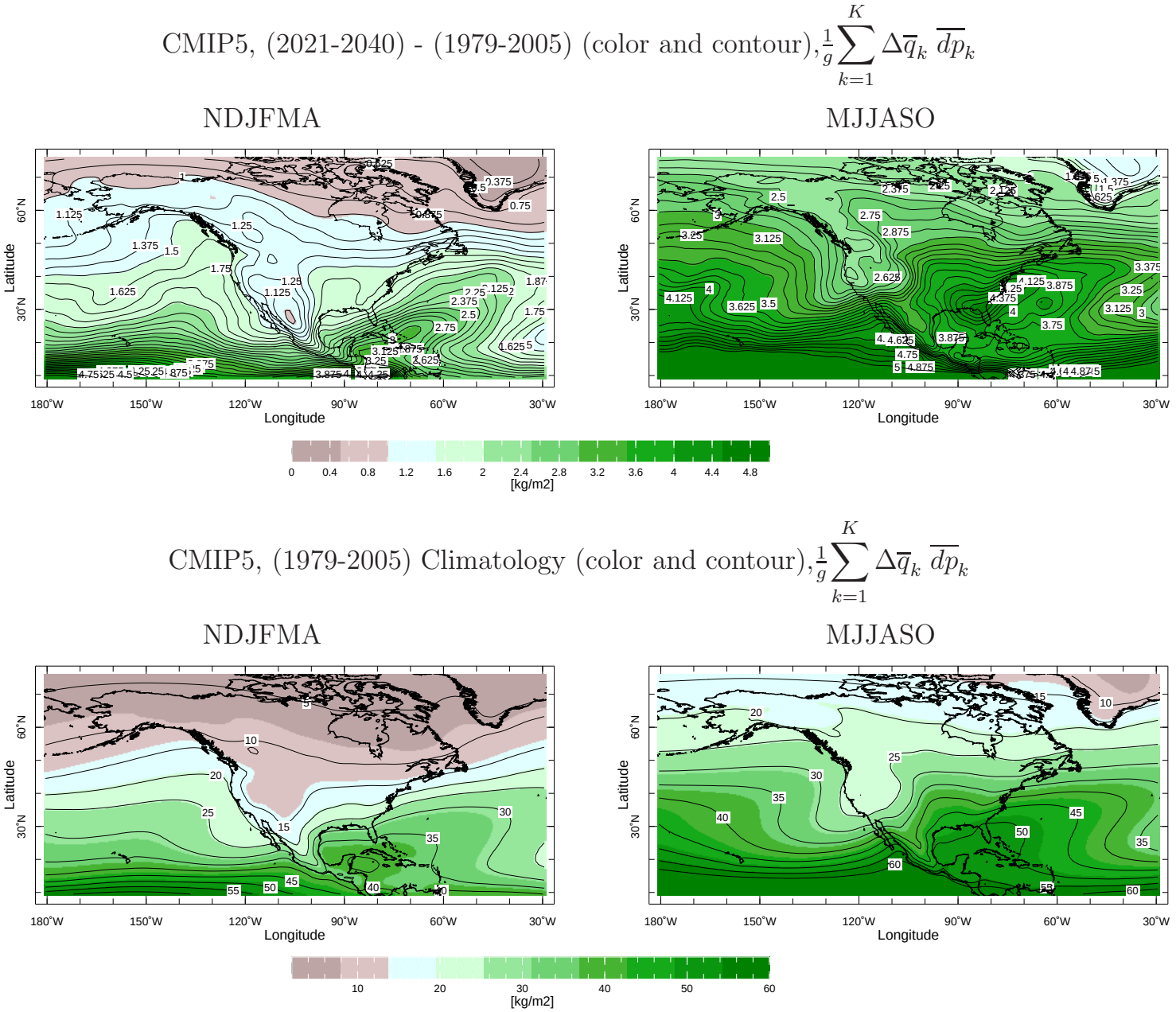

FIG. 11. The 1979-2005 to 2021-2040 change (top) and the 1979-2005 climatology (bottom) in the multimodel mean surface to 600mb vertically integrated specific humidity for the winter (left) and summer (right) half years. Units are kgm^{-2}.

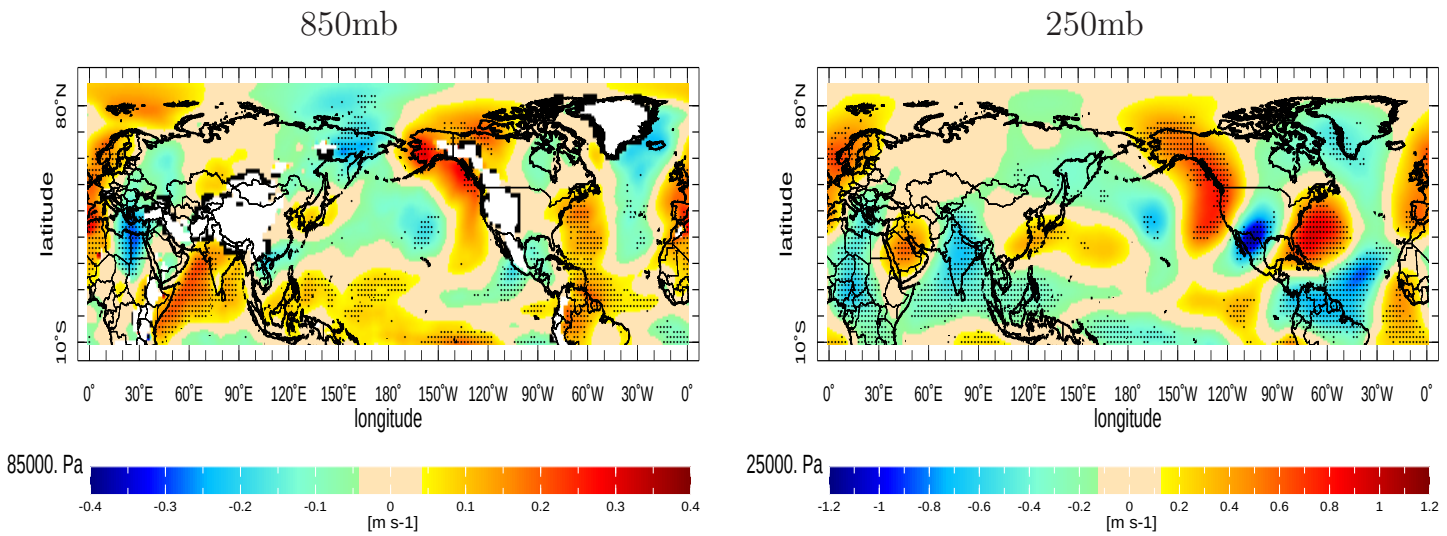

FIG. 12. The 1979-2005 to 2021-2040 change in the multimodel mean 850mb (left) and 250mb (right) meridional velocity for the winter half year. Stippling is where three quarters of models agree with the multimodel mean change. Units are ms^{-1}.